Static and Dynamic Properties of Hybridly Aligned Flexoelectric In-Plane-Switching Liquid-Crystal Display

Xiaochen Zhou,[1] Yingfei Jiang,[1] Guangkui Qin,[2] Xiaoguang Xu,[2] and Deng-Ke Yang[1,*]
[1]*Chemical Physics Interdisciplinary Program, Liquid Crystal Institute, Kent State University, Kent, Ohio 44242, USA*
[2]*BOE Technology Group Co., No. 9 Dize RD, BDA, Beijing 100171, China*
(Received 1 May 2017; revised manuscript received 18 August 2017; published 15 November 2017)

We construct a flexoelectric liquid-crystal display based on the in-plane-switching mode. The display uses a hybrid alignment cell where there are intrinsically splay and bend deformations of the liquid crystal, which promote the flexoelectric effect. In the absence of applied electric fields, the liquid crystal is aligned in a vertical plane. When a horizontal electric field is applied, the liquid crystal is azimuthally switched out of the vertical plane through the flexoelectric interaction, which is much stronger than the dielectric interaction in regular in-plane-switching displays. Also, the azimuthal rotation of the liquid crystal is sensitive to the polarity of the applied electric field. A positive field produces a counterclockwise rotation, while a negative field produces a clockwise rotation. We experimentally measure the flexoelectric coefficients and study the static and dynamic electro-optical properties of the display. We observe that the turn-on and turn-off times are linearly proportional to the inverse of the applied electric field. We also carry out theoretical and simulation studies and obtained results which agree well with the experimental results. Because the flexoelectric interaction is sensitive to the polarity of the applied voltage, both turn-on and turn-off times can be significantly reduced by applying voltages.

DOI: 10.1103/PhysRevApplied.8.054033

I. INTRODUCTION

Liquid-crystal displays are widely used in many applications from small-size smartphones to large-size TVs. The commonly used display modes are twist-nematic, vertical-alignment, in-plane-switching (IPS), fringe-field-switching (FFS), and advanced-super-dimension-switching (ADS) modes [1–9]. All of these modes utilize the dielectric interaction between the liquid crystal and the externally applied electric field E. This interaction is polarity insensitive and the aligning effect of the electric field on the liquid crystal does not change when the polarity of the applied electric field is reversed. The interaction energy is proportional to the square of the electric field E^2. One major problem with the current liquid-crystal displays is their low energy efficiency. One way to increase the energy efficiency is to use a color sequential scheme which does not need color filters, but needs a response time less than 1 ms in order to eliminate the color break. Under the dielectric interaction, the turn-on time depends on the applied voltage and can be reduced by applying higher voltages. The turn-off time, typically around 10 ms, however, only depends on the liquid-crystal configuration and cannot be reduced by applying voltages. The driving electric field E_d (to turn on the display) and the turn-off time $\tau_{\rm off}$ are approximately governed by the relation

$$\tau_{\rm off} E_d^2 = a\gamma, \tag{1}$$

where γ is the rotational viscosity coefficient and a is a constant. It should not be misunderstood by this equation that the turn-off time is independent of the applied electric field. This equation indicates that the product of the electric field needed to turn on the display and the turn-off time is a constant, and shows the trade-off between the driving electric field and the turn-off time: for a fixed viscosity coefficient, a liquid-crystal configuration with a shorter turn-off time will have a higher driving electric field. Many studies have been carried out to decrease the response time of liquid-crystal displays, including designing new modes such as blue phase display [10–13], and using polymer stabilization [14,15]. These methods can only decrease the turn-off time $\tau_{\rm off}$ to some extent, but not dramatically. Furthermore, there is a trade-off in the approaches that the driving electric field is increased as indicated by Eq. (1).

Flexoelectric interaction is different from the dielectric interaction. In some particular distorted liquid-crystal director configurations and for liquid crystals with some particular shapes, the permanent dipoles of the liquid-crystal molecules can point in the same direction and thus nonzero net electric polarization is produced. The interaction between the net polarization and an externally applied electric field is called flexoelectric interaction. This interaction energy is linearly proportional to the electric field E and is sensitive to the polarity of the applied electric field. Thus, it becomes possible to turn on

*Corresponding author.
dyang@kent.edu

the liquid-crystal display by applying a dc voltage in one direction and turn off the display by applying a dc voltage in the opposite direction. Therefore, the turn-off time can be reduced by applying voltages. Although the flexoelectric effect was discovered by Meyer almost 50 years ago [16] and observed in some display-cell geometries [17–21], it has not been used for liquid-crystal displays. Most of the flexoelectric liquid-crystal devices use short-pitch cholesteric liquid crystals in the uniform lying helix texture or uniform standing helix texture [22–29]. Sub-ms switching time has been achieved. There are, however, some problems with the cholesteric flexoelectric devices that it is difficult to achieve large uniform size, because they require a unidirectional orientation of the helical axis. The flexoelectric effect has also been observed in regular IPS and FFS displays because of the nonuniform liquid-crystal director configuration produced by nonuniform electric fields. There, instead of beneficial, the effect causes the problem of flickering [30–34]. Another way to promote the flexoelectric effect is to use hybridly aligned geometry where there are intrinsic splay and bend deformations. Some time ago, Dozov and Durand used the hybridly aligned cell to study the flexoelectric effect and measure the flexoelectric coefficient [35,36]. They also proposed to use the structure for display application [37]. Recently, Elamain *et al.* also reported a flexoelectric effect in the hybridly aligned cell with a bent-core liquid-crystal dopant which enhanced the flexoelectric effect. They observed the azimuthal rotation of the liquid crystal when the in-plane electric field was applied [38]. They analyzed the static liquid-crystal director configuration under the flexoelectric interaction. The liquid-crystal mixture used, however, had a negative dielectric anisotropy (−2.3) and the dielectric interaction also played a role in the switching. Zheng *et al.* theoretically studied the flexoelectric effect in the hybridly aligned cell [39] and made use of the geometry to measure flexoelectric coefficients [40].

In this paper, we report a study of a flexoelectric IPS liquid-crystal display based on a nematic liquid crystal doped with a liquid-crystal dimer having a large flexoelectric coefficient. Hybrid alignment of the liquid crystal is used, which is simple and can be fabricated with current mature technologies. We study the static and dynamic electro-optical behavior and achieve fast switching time.

II. PHYSICAL PROPERTIES

We first study the flexoelectric effect in a hybridly aligned liquid-crystal cell as shown in Fig. 1(a). The electrodes are on the top and bottom substrates, different from that shown in Fig. 1(a). The inner surface of the top substrate is coated with a polyvinyl alcohol (PVA) and rubbed to generate the homogeneous alignment of the liquid crystal. The inner surface of the bottom substrate is coated with a polyimide [SE1211 (Nissian Chemical)] to generate the homeotropic alignment of the liquid crystal.

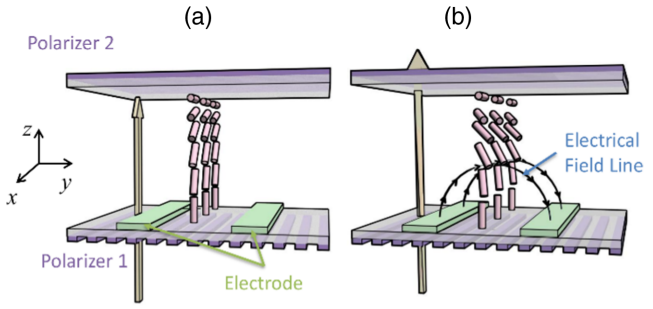

FIG. 1. Schematic diagram of the flexoelectric IPS display. (a) voltage off state, (b) voltage on state.

The cell thickness is d. The liquid-crystal director in the cell is given by

$$\vec{n} = \sin\theta(z)\hat{x} + \cos\theta(z)\hat{z}, \tag{2}$$

where the x axis is parallel to the rubbing direction of the alignment layer on the top surface, the z axis is perpendicular to the cell substrate, and θ is the angle between the liquid-crystal director and the z axis. In the absence of applied voltage, under the one elastic constant approximation ($K_{11} = K_{33} = K$), the polar angle is given by

$$\theta = \pi z/2d. \tag{3}$$

There are splay and bend deformations in this configuration. For a liquid crystal with a proper molecular structure, the deformations generate a spontaneous electric polarization given by

$$\begin{aligned}\vec{P}_f &= e_s(\vec{n}\nabla\cdot\vec{n}) + e_b(\vec{n}\times\nabla\times\vec{n}) \\ &= \left(\frac{\pi}{2d}\right)\left[-(e_s\sin^2\theta + e_b\cos^2\theta)\hat{x}\right. \\ &\quad \left. -\frac{1}{2}(e_s - e_b)\sin 2\theta\hat{z}\right],\end{aligned} \tag{4}$$

where e_s is the splay flexoelectric coefficient and e_b is the bend flexoelectric coefficient.

In our experiment, the liquid crystals used are mixtures of a regular positive nematic liquid crystal (LC) MAT-11-575 (Merck), a regular negative nematic LC ZLI-4330 (Merck), and a liquid-crystal dimer CB7CB [41–43] whose chemical structure is shown in Fig. 2(a). Different from the regular rodlike liquid-crystal molecules, CB7CB had two rigid segments on the two sides and a flexible linkage in the middle. The flexible linkage has an odd number of carbons and exhibits a bent structure as shown in Fig. 2(b), and is known to exhibit a large flexoelectric coefficient [44–47]. The dielectric anisotropy of the mixture is close to 0 such that the dielectric interaction is negligible.

The induced electric polarization generates bound electric charges on the cell surfaces, which produces a voltage. We use the SawyerTower circuit [48–50] to measure the

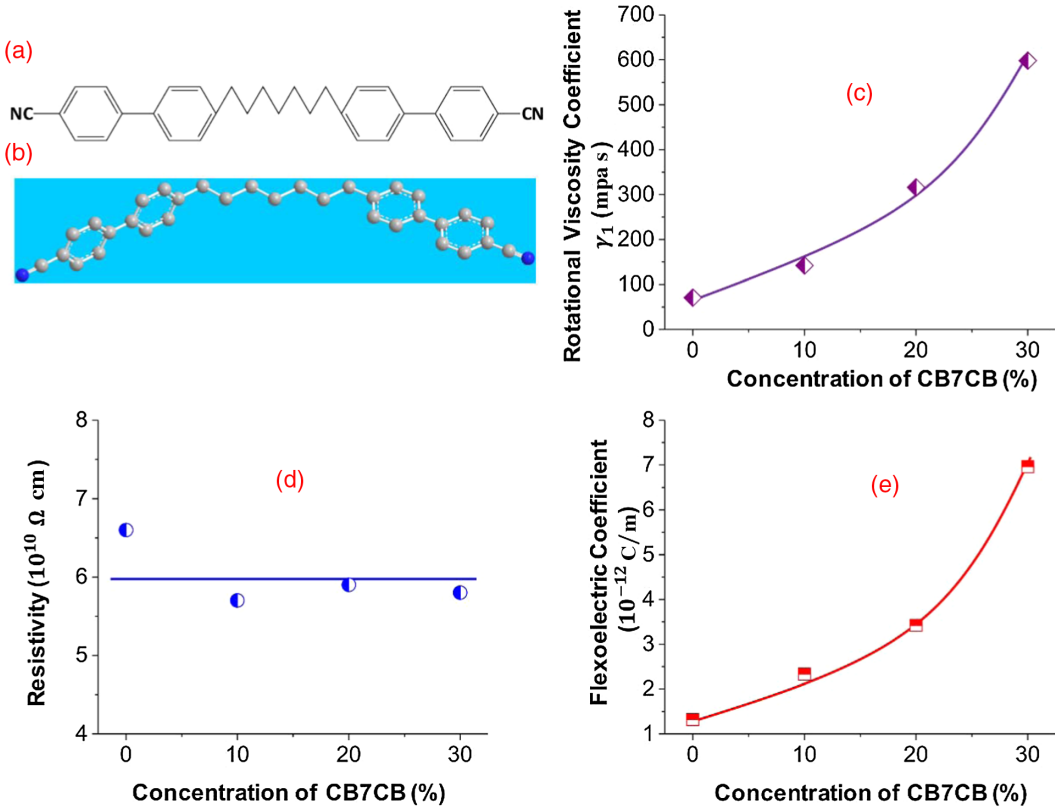

FIG. 2. (a) Chemical structure of CB7CB and (b) energy-minimized molecular configuration calculated from Chem3D Pro. (c) Rotational viscosity coefficient vs CB7CB concentration. (d) Resistivity vs CB7CB concentration. (e) Flexoelectric coefficient e_s-e_b vs CB7CB concentration. The lines are a guide to the eye.

electric polarization induced by the deformations in the liquid-crystal cell (details are given in the Supplemental Material [51]). In the experiment, a triangular voltage wave with the amplitude of 3 V and frequency of 50 Hz is used. The liquid crystal does not change orientation under the voltage. The measured flexoelectric coefficient $(e_s$-$e_b)$ is shown in Fig. 2(e). It increases dramatically with the CB7CB concentration c. This large flexoelectric coefficient helps to provide evidence supporting our conclusion on the flexoelectric effect in our designed display.

The orientation of the liquid-crystal molecules depends on the internal electric field that is the sum of the external electric field and the electric field produced by ions inside the material. In order to see whether there are ions inside the material, we measure the resistivity of the material. The result is shown in Fig. 2(d). The resistivity remains quite high, almost independent of the CB7CB concentration. Based on this result, we can rule out of the effect of ions.

III. DISPLAY

In our flexoelectric display, the liquid-crystal cell consists of two parallel substrates where the top substrate is coated and rubbed for homogeneous alignment of the liquid crystal and the bottom one is coated with a homeotropic alignment layer as shown in Fig. 1. The bottom substrate is patterned with interdigitated electrodes as in IPS cells. The alignment layer rubbing direction makes the angle of 10° with respect to the stripe electrodes. The nematic liquid crystal is filled into the cell. The cell is sandwiched between two crossed polarizers. The top polarizer (polarizer 2) is perpendicular to the alignment layer rubbing direction. The transmission axis of the bottom polarizer (polarizer 1) is orthogonal to that of the top polarizer.

In the voltage off state, the liquid crystal lies in the xz plane as shown in Fig. 1(a). The incident light has the polarization parallel to the x axis. When the light propagates through the liquid-crystal layer, its polarization does not change and thus is absorbed by the top polarizer. In this state, there are splay and bend deformations, because of the hybrid alignments of the cell. This deformation induces a spontaneous electric polarization as discussed before. When a voltage is applied across the IPS electrodes, an electric field $\vec{E} = E_y\hat{y} + E_z\hat{z}$ on the yz plane is generated, as shown in Fig. 1(b). The liquid-crystal mixtures used have very small dielectric anisotropies (measured to be −0.1) and, therefore, the dielectric interaction energy is negligible. The free energy of the system consists of the elastic free energy and the flexoelectric interaction free energy. The free-energy density is given by

$$f = f_{\text{elastic}} + f_{\text{flexoelectric}}. \tag{5}$$

When a voltage is applied across the IPS electrodes, the generated electric field exerts a torque on the liquid-crystal molecules, which rotates the liquid-crystal molecules out of the xz plane. The liquid-crystal director is described by

$$\vec{n} = \sin\theta(z)\cos\varphi(z)\hat{x} + \sin\theta(z)\sin\varphi(z)\hat{y} + \cos\theta(z)\hat{z}, \tag{6}$$

where θ and φ are the polar and azimuthal angle of the liquid-crystal director. The flexoelectric interaction energy is

$$f_{\text{flexoelectric}} = -\vec{P}_f \cdot \vec{E} = \left[\sin\varphi(e_b\cos^2\theta + e_s\sin^2\theta)\theta' + \frac{1}{2}e_b\sin 2\theta\cos\varphi\varphi'\right]E_y - \frac{1}{2}[(e_b - e_s)\sin 2\theta\theta']E_z, \tag{7}$$

where $\theta' = \partial\theta/\partial z$ and $\varphi' = \partial\varphi/\partial z$ are the derivatives. Note that the interaction energy is linearly proportional to E, different from the dielectric interaction where the interaction energy is proportional to E^2. In the regions between the electrodes, the generated electric field is mainly in the horizontal direction (the y direction). For a positive E_y, the flexoelectric interaction will rotate the liquid crystal counterclockwise. For a negative E_y, the flexoelectric interaction will rotate the liquid crystal clockwise. When the liquid crystal is rotated out of the electrode plane, it is no longer parallel to the polarization of the incident light. When the light propagates through the liquid-crystal layer, its polarization changes and thus passes the top polarizer, as shown in Fig. 1(b).

We first carry out a simulation study of the display. The equilibrium state of the liquid crystal is calculated by minimizing the free energy of the system and the results are shown in Fig. 3. The following parameters are used in the simulation. The electrode width and gap are both 7.5 μm. The cell thickness is 3 μm. The elastic constants are $K_{11} = 8.2$ pN, $K_{22} = 5.0$ pN, $K_{33} = 10.0$ pN. The dielectric constant is $\Delta\varepsilon = -0.1$, and the flexoelectric coefficient is $e_s + e_b = 10$ pC/m (a typical value). The angle between the electrode stripes and the aligning direction of the homogeneous alignment layer is 10°. When the applied voltage is 0 V, the liquid-crystal director lies in the xz plane as shown in Fig. 3(a). When 15 V is applied, the liquid-crystal director configuration is shown in Fig. 3(b). Now the liquid crystal is rotated toward the y direction. The calculated twist angle as a function of the horizontal axis y is shown in Fig. 3(c). The twisting direction of the liquid crystal depend on the direction of the electric field. In the region where the electric field points to $+\hat{y}$, the liquid crystal twists in one direction, while in the region where the electric field points to $-\hat{y}$, the liquid crystal twists in the opposite direction. This means the design has an intrinsic two-domain structure and, therefore, the display has a large viewing angle. The asymmetry of the curve is caused by the nonzero angle between the electrode stripe and the aligning direction of the alignment layer.

We then perform experimental studies of the display. The width and gap of the electrode are all 7.5 μm (the same as in the simulation study). The bottom substrate is coated with a homeotropic alignment layer SE-1211 and the top substrate is coated with a homogenous alignment layer PVA and rubbed. Although the flexoelectric IPS cell did not require a nonzero deviation rubbing angle, the rubbing direction used here is 10° deviated from the electrode line, which is the same as that in the current IPS display manufacturing. The cell thickness is controlled by 3 μm (or 5 μm) spherical spacers. Three mixtures are constructed from LC MAT-11-575, LC ZLI-4330 (Merck), and LC dimer CB7CB. In order to measure their dielectric anisotropies, the mixtures are filled into homeotropic cells with regular top and bottom electrodes. ac voltages with a 1-kHz frequency are used to measure the capacitances of the cells. When a low voltage is applied, the liquid crystal is perpendicular to the cell substrate and the capacitance of the cell is proportional to $\varepsilon_\parallel$. When a sufficiently high voltage is applied, the liquid crystal is parallel to the substrates, because of the negative dielectric anisotropy, and the capacitance of the cell is proportional to $\varepsilon_\perp$. The dielectric anisotropy is calculated from $\varepsilon_\parallel$ and $\varepsilon_\perp$. The results are also listed in Table I and all the mixtures constructed have very small negative dielectric anisotropies. The mixtures have melting temperatures lower than 20 °C and a nematic-isotropic transition temperature higher than 82 °C.

The display is first studied under a polarizing optical microscopy with crossed polarizers. The microphotographs

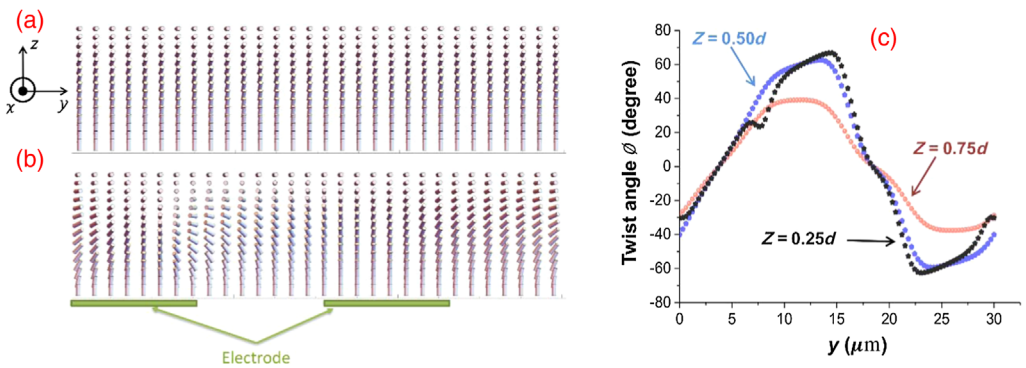

FIG. 3. (a) Simulated liquid-crystal director profile under 0 V. (b) Simulated liquid-crystal director profile under 15 V. (c) Twist angle as a function of the horizontal coordinate y at various z positions under 15 V.

TABLE I. The materials concentration and dielectric anisotropy of the three mixtures used in the experiment.

	ZLI-4330	MAT-11-575	CB7CB	$\Delta\varepsilon$	Δn	Flexoelectric coefficient $(e_s\text{-}e_b)$ $(10^{-12}$ C/m)	Resistivity $(10^8\ \Omega$m)	Rotational viscosity coefficient (mPa s)
Mixture 1	75%	15%	10%	−0.14	0.141	+2.22	5.7	142
Mixture 2	70%	10%	20%	−0.04	0.142	+3.42	5.9	318
Mixture 3	70%	0%	30%	−0.17	0.144	+6.96	5.8	598

of the display are shown in Fig. 4, where mixture 3 is used. In the absence of voltage, the display appears dark as shown in Fig. 4(a), indicating there is no polarization rotation effect in the cell. When the voltage is increased, the regions between the electrodes become brighter. We do not observe any electroconvection or turbulence effect, confirming that the transmittance change is caused by the flexoelectric-effect-induced reorientation of the liquid crystal.

The electro-optical properties of the flexoelectric IPS display are measured by using a green laser at the wavelength 543.5 nm. The transmission-voltage curves are measured for two sets of cells with different gaps for each mixture under dc voltage and are shown in Fig. 5. The maximum transmission of the cells is 100% when normalized to that of the two parallel polarizers. At 0 V/μm, the transmittance is 0. As the applied electric field is increased, the transmittance increases. When the concentration of CB7CB is increased, the transmittance increases faster with the applied voltage, agreeing with the observed result that the flexoelectric coefficient increases with the CB7CB concentration as shown in Fig. 2(c). Note that the maximum transmittance of the regular IPS display with equal electrode width and gap is about 40%. The maximum transmittance obtained here is about 35%. The dependence of the transmittance on the applied voltage is not straightforward in these cells, because both the polar and azimuthal angles change with position in the light-propagation direction. Near the bottom of the cell, the orientation of the liquid-crystal director is close to the light-propagation direction, and the effective birefringence is small and thus the Mauguin condition for the waveguide effect is not satisfied and the polarization of the incident light does not simply rotate with the liquid-crystal director. When the light propagates through the liquid crystal, its polarization is changed from linear polarization to elliptical polarization. The transmittance can only be calculated numerically. An interesting phenomenon is the crossover of the transmittance vs voltage curves of mixtures 2 and 3. Further simulation studies are needed in order to explain it.

We also study the dynamic behavior of the flexoelectric IPS display. Under the flexoelectric interaction, the turn-on time can be reduced by applying a positive voltage and the turn-off time can also be reduced by applying a negative voltage. We measure the switching times under a variety of applied electric voltages and the results are shown in Fig. 6.

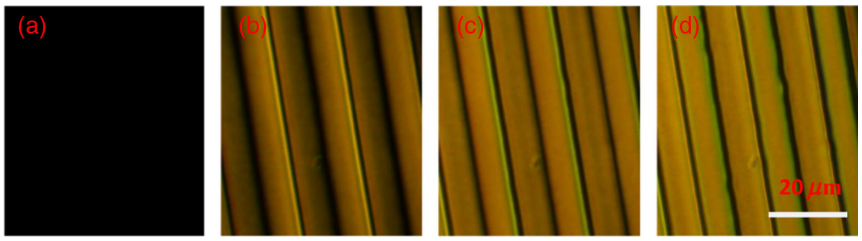

FIG. 4. Microphotographs of the nematic flexoelectric IPS display under various dc voltages. (a) 0 V, (b) 10 V, (c) 15 V, (d) 20 V.

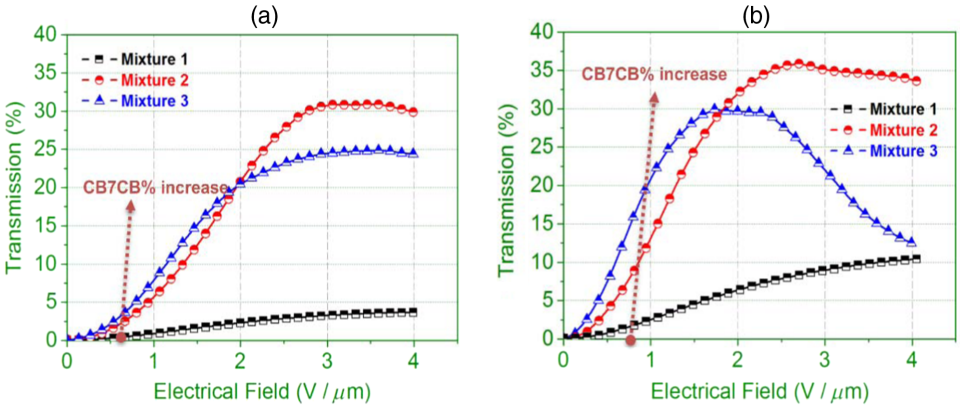

FIG. 5. Transmittance vs applied electric field. Cell thickness: (a) 3 μm, (b) 5 μm.

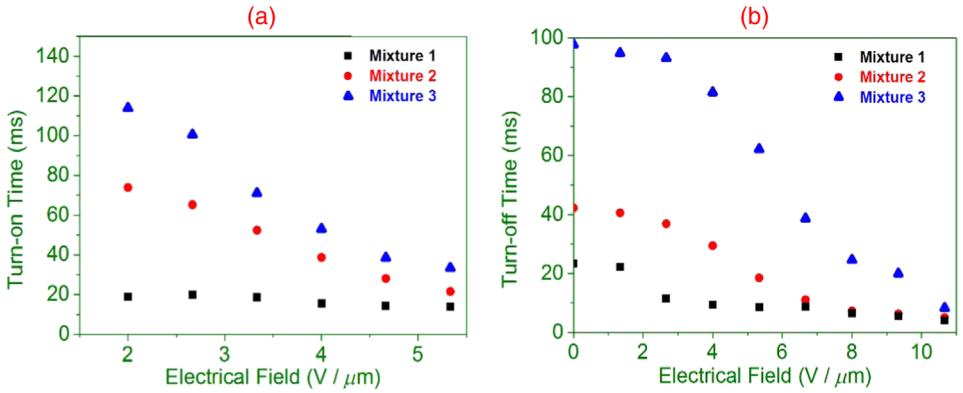

FIG. 6. Switching time vs applied electric field of the flexoelectric IPS display with the cell thickness of 3 μm. (a) turn-on time, (b) turn-off time.

In the measurement of the turn-on time, a positive dc voltage is applied, which generates a positive electric field. After the voltage is turned on, the transmittance increases with time and then saturates at a maximum value (shown in Fig. 5). The turn-on time is the time for the transmittance changed from 10% to 90% of the maximum transmittance. The results of the 3-μm cells are shown in Fig. 6(a). For all the samples, the turn-on time decreases when the applied electric field is increased. In the measurement of the turn-off time, first the positive voltage for the maximum transmittance is applied and then a reversed polarity dc voltage is applied. This is different from the measurement of turn-off time of regular displays utilizing the dielectric interaction, where the applied electric field is simply removed. The turn-off time is the time for the transmittance changed from 90% to 10% of the maximum transmittance. The results of the 3-μm cells are shown in Fig. 6(b). For all the samples, the turn-off time decreases when the applied field in the opposite direction is increased. This confirms that the interaction is flexoelectricity. In the above section, it is shown that the driving electric field decreases with increasing CB7CB concentration, due to the increment of the flexoelectric coefficient. Conversely, both the turn-on and turn-off times increase with the CB7CB concentration. This is due to the fact that the viscosity coefficient increases dramatically with the CB7CB concentration, because it is a big molecule (about twice as long as regular liquid-crystal molecules). We measure the rotational viscosity coefficient of the mixtures. In the measurement, only the positive nematic LC MAT-11-575 and the liquid-crystal dimer CB7CB are used to construct mixtures that are used to make the regular IPS displays. The turn-off time of the IPS displays are measured and the rotational viscosity coefficient is calculated. The result is shown in Fig. 2(c) and Table I. When the concentration is increased from 0% to 30%, the viscosity coefficient became 8 times larger. Nevertheless, in the flexoelectric IPS display, the turn-off time is decreased from 98 to 8.3 ms, which is 11 times faster, when the electric field in the opposite direction is increased from 0 to 10 V/μm. Here, we only demonstrate the operation principle of flexoelectric IPS liquid-crystal display but have not yet optimized its performance. We believe the driving voltage and response time can be improved greatly with the usage of proper materials with lower viscosities and higher flexoelectric coefficients.

IV. THEORETICAL CONSIDERATION

Although a precise analytical analysis of the liquid-crystal configuration and optical property is very difficult, we do a theoretical analysis with some approximations to show the electric-field dependence of the switching times. The electric field generated by the IPS electrode is mainly parallel to the cell substrate. As an approximation, we neglect the electric field in the vertical direction (perpendicular to the cell substrate). $E_y = E$ and $E_z = 0$. The free-energy density (flexoelectric interaction energy and elastic energy) is given by

$$f = \left[(e_b\cos^2\theta + e_s\sin^2\theta)\sin\varphi\theta' + \frac{1}{2}e_b\sin 2\theta\cos\varphi\varphi'\right]E + \frac{1}{2}K\theta'^2 + \frac{1}{2}K\sin^2\theta\varphi'^2, \quad (8)$$

where the one elastic constant approximation ($K_{11} = K_{22} = K_{33} = K$) is used. Using the Euler-Lagrange equation to minimize the free energy with respect to θ and φ, we obtain

$$-\frac{\delta f}{\delta\theta} = K\theta'' + (e_s + e_b)E\sin^2\theta\cos\varphi\varphi' - K\sin\theta\cos\theta\varphi'^2 = 0. \quad (9)$$

$$-\frac{\delta f}{\delta\varphi} = K\sin^2\theta\varphi'' + 2K\sin\theta\cos\theta\theta'\varphi' - E(e_b + e_s)\sin^2\theta\cos\varphi\theta' = 0. \quad (10)$$

When the applied electric field is low, the azimuthal angle is small, and the polar angle remains as $\theta = \pi z/2d$. The above two equations become

$$(e_s + e_b)E\sin^2\theta\cos\varphi - K\sin\theta\cos\theta\varphi' = 0. \quad (11)$$

$$K\sin^2\theta\varphi'' + \frac{K\pi}{d}\sin\theta\cos\theta\varphi' - \frac{\pi}{2d}E(e_b + e_s)\sin^2\theta\cos\varphi = 0. \quad (12)$$

Substituting Eq. (11) into Eq. (12), we have

$$K\sin^2\theta\varphi'' + \frac{\pi}{2d}(e_s + e_b)E\sin^2\theta\cos\varphi = 0. \quad (13)$$

When φ is small, we use the approximation $\cos\varphi = 1$, and the solution to the above equation is

$$\varphi = -\frac{\pi}{4Kd}E(e_b + e_s)z^2 + Az + B, \quad (14)$$

where A and B are integration constants. Now let us consider the boundary conditions to determine the integration constants. At $z = d$ the liquid crystal is anchored along the x direction by the rubbed alignment layer, and the boundary condition is $\varphi(z = d) = 0$. At $z = 0$ the liquid crystal is anchored homeotropically (along the z direction) by the homeotropic alignment layer and the polar angle θ is zero. The liquid crystal is free to rotate azimuthally, and the boundary condition is $\varphi' = 0$. Using these two boundary conditions we get

$$\varphi = -\frac{\pi}{4Kd}E(e_b + e_s)(z^2 - d^2). \quad (15)$$

This electric-field-induced transition of the liquid crystal is thresholdless, agreeing with the experimental result shown in Fig. 5.

Now, we consider the dynamics of the rotation of the liquid crystal. The dynamic equation of the azimuthal rotation of the liquid crystal can be obtained by balancing the viscosity torque and the torque produced by the flexoelectric interaction and elastic deformation:

$$\gamma\frac{\partial\varphi}{\partial t} = -\frac{\delta f}{\delta\varphi} = K\sin^2\theta\varphi'' + \frac{\pi}{2d}E\sin^2\theta(e_b + e_s), \quad (16)$$

where γ is the rotational viscosity coefficient of the liquid crystal. We first consider the turn-on time. Initially, the applied field is 0 and the azimuthal angle $\varphi(t = 0) = 0$. At $t = 0$, the applied voltage is changed to $E_{\rm on}$. Because of the boundary conditions, the azimuthal angle is

$$\varphi = -a(t)(z^2 - d^2), \quad (17)$$

where $a(t)$ is the amplitude that varies with time. Considering the dynamics at the middle plane of the cell $(z = d/2)$, $\sin^2\theta = 1/2$, Eq. (16) becomes

$$\gamma\frac{3}{4}d^2\frac{\partial a}{\partial t} = -Ka + \frac{\pi}{4d}E_{\rm on}(e_b + e_s). \quad (18)$$

The solution to the above equation is

$$a = \frac{\pi}{4dK}E_{\rm on}(e_b + e_s)(1 - e^{-t/\tau_o}), \quad (19)$$

where $\tau_o = 3\gamma d^2/4K$. In the state with 0 transmittance, the azimuthal angle is $\varphi_{0\%} = 0$ and the corresponding value of a is 0. In the state with the maximum transmittance, the azimuthal angle at the middle plane is $\varphi_{100\%}$ and the corresponding value of a is $(4/3d^2)\varphi_{100\%}$. The azimuthal angles of the states with 10% and 90% of the maximum transmittances are $\varphi_{10\%}$ and $\varphi_{90\%}$, respectively. The turn-on time is the time interval for the transmittance to increase from 10% to 90% of the maximum transmittance. It can be obtained

$$\tau_{\rm on} = \tau_o\ln\left[\left(1 - \frac{16K\varphi_{10\%}}{3\pi dE_{\rm on}(e_b + e_s)}\right)\Big/\left(1 - \frac{16K\varphi_{90\%}}{3\pi dE_{\rm on}(e_b + e_s)}\right)\right]. \quad (20)$$

When $\{[16K\varphi_{90\%}]/[3\pi dE_{\rm on}(e_b + e_s)]\} \ll 1$ (note $\varphi_{10\%} < \varphi_{90\%}$), namely, the applied electric field is high, then

$$\tau_{\rm on} \approx \tau_o\frac{16K(\varphi_{90\%} - \varphi_{10\%})}{3\pi dE_{\rm on}(e_b + e_s)} = \frac{4\gamma d}{(e_b + e_s)E_{on}}\left(\frac{\varphi_{90\%} - \varphi_{10\%}}{\pi}\right). \quad (21)$$

The reciprocal of the turn-on time is proportional to the applied electric field $E_{\rm on}$. Now, we consider the turn-off time. Initially, the liquid crystal is in the state with the maximum transmittance and the azimuthal angle is $\varphi = -4\varphi_{100\%}(z^2 - d^2)/3d^2$. At $t = 0$ the applied voltage is changed to $E_{\rm off}$ in the reversed direction. The dynamic equation at the middle plane of the cell $(z = d/2)$ is

$$\gamma\frac{3}{4}d^2\frac{\partial a}{\partial t} = -Ka - \frac{\pi}{4d}E_{\rm off}(e_b + e_s). \quad (22)$$

Initially, $a = 4\varphi_{100\%}/3d^2$. The solution to the above equation is

$$a = \left[\frac{4\varphi_{100\%}}{3d^2} + \frac{\pi}{4dK}(e_b + e_s)E_{\rm off}\right]e^{-t/\tau_o} - \frac{\pi}{4dK}(e_b + e_s)E_{\rm off}. \quad (23)$$

The turn-off time is the time interval for the transmittance to decrease from 90% to 10% of the maximum transmittance. It can be obtained

$$\tau_{\rm off} = \tau_o\ln\left[\left(\frac{4\varphi_{90\%}}{3d^2} + \frac{\pi}{4dK}(e_b + e_s)E_{\rm off}\right)\Big/\left(\frac{4\varphi_{10\%}}{3d^2} + \frac{\pi}{4dK}(e_b + e_s)E_{\rm off}\right)\right]. \quad (24)$$

If the applied electric field in the reversed direction is 0, the turn-off time is

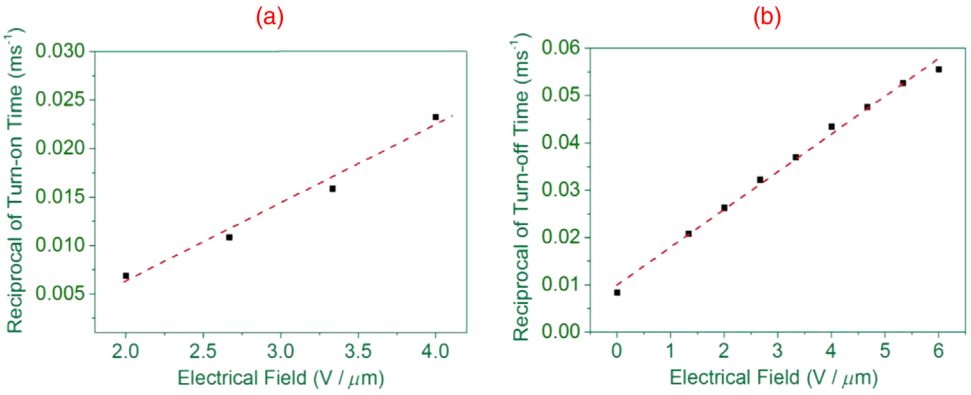

FIG. 7. Reciprocal of (a) turn-on and (b) turn-off time vs applied electric field of the flexoelectric IPS display filled with mixture 3. The black dot is measured data and the red dashed line is the fitting curve.

$$\tau_{\rm off} = \tau_o \ln(\varphi_{90\%}/\varphi_{10\%}). \tag{25}$$

If $E_{\rm off}$ is large, then $\{[16K\varphi_{90\%}]/[3\pi d E_{\rm off}(e_b+e_s)]\} \ll 1$, and

$$\tau_{\rm off} \approx \tau_o \frac{4\gamma d}{(e_b+e_s)E_{\rm off}}\left(\frac{\varphi_{90\%}-\varphi_{10\%}}{\pi}\right). \tag{26}$$

The reciprocal of the turn-off time is proportional to the applied electric field $E_{\rm off}$.

We plot the reciprocal of the experimentally measured turn-on time of the cell with mixture 3 as a function of the applied electric field in Fig. 7(a). The slope of the $1/\tau_{\rm on}$ vs $E_{\rm on}$ line is 8.1×10^{-3} μm/(ms V). From Eq. (21) we see the slope is $[(e_b+e_s)/4\gamma d][\pi/(\varphi_{90\%}-\varphi_{10\%})]$. The rotational viscosity coefficient γ is 598×10^{-3} Pa s and the cell thickness d is 3 μm. The precise values of the azimuthal angles for the various transmittances are unknown, because of the complex liquid-crystal configuration. As an approximation we use $\varphi_{100\%}=-\pi/4$, $\varphi_{90\%}=-(90\%/100\%)\pi/4$, and $\varphi_{10\%}=-(10\%/100\%)\pi/4$. Therefore, $(e_b+e_s)=-11.8\times10^{-12}$ C/m. The flexoelectric coefficients (e_s-e_b) measured by the Sawyer-Tower method is $+6.96\times10^{-12}$ C/m. Therefore, $e_b=-9.3\times10^{-12}$ C/m and $e_s=-2.5\times10^{-12}$ C/m. These values are reasonable, because the flexoelectric coefficients are mainly contributed by the dimer component CB7CB, which has a bent shape, in the mixture. The mixture contains 30% CB7CB. For the pure CB7CB system, the flexoelectric coefficient would be about $e_b=-31\times10^{-12}$ C/m, which is close to the value reported by Varanytsia and Chien [52]. We also plot the inverse of the experimentally measured turn-off time as a function of the applied electric field with opposite polarity in Fig. 7(b). The slope is 8.0×10^{-3} μm/(ms V). Using Eq. (26), the same flexoelectric coefficients are obtained.

V. DISCUSSION AND SUMMARY

We studied the electro-optical properties of a flexoelectric IPS display. The switching of the display is achieved through flexoelectric interaction which is sensitive to the polarity of the applied voltage. We demonstrate that both the turn-on and turn-off time can be dramatically reduced by applying voltages. The dimer dopant used in our study exhibits a large flexoelectric effect but has a high-viscosity coefficient which is undesirable and must be improved. With better flexoelectric liquid crystal developed in the future, the display will have sub-ms switching time. Two of the important issues in display manufacturing are the electrode and alignment layer. The display we designed uses the same electrode as in the regular IPS display. It uses a hybrid of alignment layers: one side of the cell has a homogeneous alignment layer and the other side has a homeotropic alignment layer. Homogeneous alignment layers and homeotopric alignment layers as well as the IPS electrode are well-developed technologies and widely used in current mainstream manufacturing. Two important features of display are the contrast ratio and viewing angle. First, in the dark state of this alternate display, the liquid crystal is aligned in a plane parallel to the polarizer. There is no light leakage for normal incident light, and thus the display will have a very high contrast ratio. Second, the display intrinsically has a two-domain structure and exhibits self-compensation, and therefore has a good viewing angle.

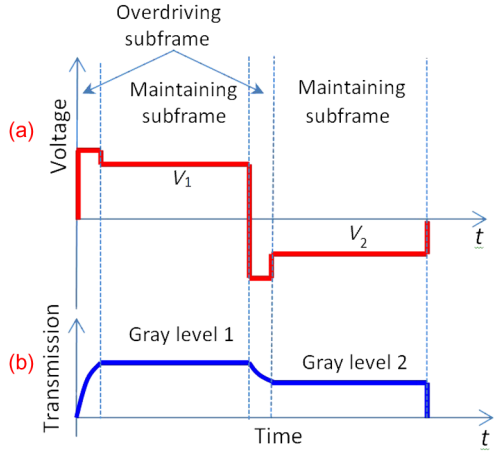

FIG. 8. Schematic diagram of the drive scheme for the reduction of transition time. (a) applied voltage and (b) transmission.

In addressing the display utilizing flexoelectric interaction, the driving scheme shown in Fig. 8 can be used. It consists of a maintaining subframe and an overdriving subframe. In the maintaining subframe, a voltage corresponding to the desired transmittance gray level is applied. In the overdriving subframe, a voltage with a high amplitude is applied to reduce the transition time. No matter whether the next gray level is higher or lower, a high voltage can always be used to reduce the transition time, which is impossible for displays utilizing the dielectric interaction. The polarity of the applied voltage is reserved from one frame to the next frame in order to prevent electrochemical deteriorations.

In summary, we constructed a flexoelectric IPS display with a nematic liquid crystal doped with a dimer. The dimer greatly enhances the flexoelectric effect. The display has a simple structure and uses hybrid alignment which is easy to implement in manufacturing. This technology may have an impact on liquid-crystal display. We demonstrate that the turn-off time can be reduced by a factor of 10 when a reversed voltage is applied. If a flexoelectric liquid crystal with a viscosity similar to that of regular nematic liquid crystals is developed in the future, the display would have a sub-ms response time with the help of applied voltages, and, thus, be suitable for color sequential operation.

ACKNOWLEDGMENTS

The project is supported by BOE Technology Group Co., Ltd., China.

[1] D.-K. Yang and S.-T. Wu, *Fundamentals of Liquid Crystal Devices*, 2nd ed. (John Wiley & Sons, Ltd, Chichester, U.K., 2014).
[2] M. Schadt and W. Helfrich, Voltage-dependent optical activity of a twisted nematic liquid crystal, Appl. Phys. Lett. **18**, 127 (1971).
[3] M. F. Schiekel and K. Fahrenschon, Deformation of nematic liquid crystals with vertical orientation in electrical fields, Appl. Phys. Lett. **19**, 391 (1971).
[4] R. A. Soref, Transverse field effects in nematic liquid crystals, Appl. Phys. Lett. **22**, 165 (1973).
[5] R. A. Soref, Field effects in nematic liquid crystals obtained with interdigital electrodes, J. Appl. Phys. **45**, 5466 (1974).
[6] S. H. Lee, S. L. Lee, and H. Y. Kim, Electro-optic characteristics and switching principle of a nematic liquid crystal cell controlled by fringe-field switching, Appl. Phys. Lett. **73**, 2881 (1998).
[7] E. Lueder, *Liquid Crystal Displays* (John Wiley & Sons, Ltd, Chichester, U.K., 2010).
[8] M. Oh-e and K. Kondo, Electro-optical characteristics and switching behavior of the in-plane switching mode, Appl. Phys. Lett. **67**, 3895 (1995).
[9] M. Oh-e and K. Kondo, Response mechanism of nematic liquid crystals using the in-plane switching mode, Appl. Phys. Lett. **69**, 623 (1996).
[10] H. Kikuchi, M. Yokota, Y. Hisakado, H. Yang, and T. Kajiyama, Polymer-stabilized liquid crystal blue phases, Nat. Mater. **1**, 64 (2002).
[11] Z. Ge, L. Rao, S. Gauza, and S.-T. Wu, Modeling of blue phase liquid crystal displays, J. Disp. Technol. **5**, 250 (2009).
[12] Y. Haseba, H. Kikuchi, T. Nagamura, and T. Kajiyama, Large electro-optic Kerr effect in nanostructured chiral liquid-crystal composites over a wide temperature range, Adv. Mater. **17**, 2311 (2005).
[13] Y. Chen, D. Xu, S.-T. Wu, S. Yamamoto, and Y. Haseba, A low voltage and submillisecond-response polymer-stabilized blue phase liquid crystal, Appl. Phys. Lett. **102**, 141116 (2013).
[14] X. Zhou, G. Qin, Y. Dong, and D.-K. Yang, Fast switching and high-contrast polymer-stabilized IPS liquid crystal display, J. Soc. Inf. Disp. **23**, 333 (2015).
[15] D.-K. Yang, Y. Cui, H. Nemati, X. Zhou, and A. Moheghi, Modeling aligning effect of polymer network in polymer stabilized nematic liquid crystals, J. Appl. Phys. **114**, 243515 (2013).
[16] R. B. Meyer, Piezoelectric Effects in Liquid Crystals, Phys. Rev. Lett. **22**, 918 (1969).
[17] F. Castles, S. M. Morris, D. J. Gardiner, Q. M. Malik, and H. J. Coles, Ultra-fast-switching flexoelectric liquid-crystal display with high contrast, J. Soc. Inf. Disp. **18**, 128 (2010).
[18] J. S. Patel and R. B. Meyer, Flexoelectric Electro-Optics of a Cholesteric Liquid Crystal, Phys. Rev. Lett. **58**, 1538 (1987).
[19] P. Rudquist, *The Flexoelectro-optic effect in cholesteric liquid crystals*, (Chalmers University of Technology, Göteborg, 1997).
[20] H. Chen, F. Peng, M. Hu, and S.-T. Wu, Flexoelectric effect and human eye perception on the image flickering of a liquid crystal display, Liq. Cryst. **42**, 1730 (2015).
[21] S.-W. Oh, J.-H. Park, J.-H. Lee, and T.-H. Yoon, Elimination of image flicker in a fringe-field switching liquid crystal display by applying a bipolar voltage wave, Opt. Express **23**, 24013 (2015).
[22] L. Komitov, S. T. Lagerwall, B. Stebler, and A. Strigazzi, Sign reversal of the linear electro-optic effect in the chiral nematic phase, J. Appl. Phys. **76**, 3762 (1994).
[23] H. Coles, S. Morris, F. Castles, D. Gardiner, and Q. Malik, Ultrafast high optical contrast flexoelectric displays for video frame rates, SID Symp. Dig. Tech. Pap. **43**, 544 (2012).
[24] F. Castles, S. M. Morris, and H. J. Coles, Flexoelectro-optic properties of chiral nematic liquid crystals in the uniform standing helix configuration, Phys. Rev. E **80**, 031709 (2009).
[25] P. Rudquist, L. Komitov, and S. T. Lagerwall, Volume-stabilized ULH structure for the flexoelectro-optic effect and the phase-shift effect in cholesterics, Liq. Cryst. **24**, 329 (1998).
[26] P. Rudquist, M. Buivydas, L. Komitov, and S. T. Lagerwall, Linear electro-optic effect based on flexoelectricity in a cholesteric with sign change of dielectric anisotropy, J. Appl. Phys. **76**, 7778 (1994).
[27] B. I. Outram and S. J. Elston, Frequency-dependent dielectric contribution of flexoelectricity allowing control of state switching in helicoidal liquid crystals, Phys. Rev. E **88**, 012506 (2013).

[28] B. I. Outram and S. J. Elston, Alignment of cholesteric liquid crystals using the macroscopic flexoelectric polarization contribution to dielectric properties, Appl. Phys. Lett. **103**, 141111 (2013).
[29] B. I. Outram and S. J. Elston, Flexoelectric and dielectric in-plane switching behaviour of Grandjean liquid-crystal structures, Europhys. Lett. **99**, 37007 (2012).
[30] H. S. Choi, J. H. Kim, H. G. Ham, Y. J. Lim, J. M. Lee, H. S. Jin, R. Manda, M. S. Kim, D.-K. Yang, and S. H. Lee, Studies on flickering in low frequency driven fringe-field switching (FFS) liquid crystal display, SID Symp. Dig. Tech. Pap. **47**, 1610 (2016).
[31] M. S. Kim, P. J. Bos, D.-W. Kim, D.-K. Yang, J. H. Lee, and S. H. Lee, Flexoelectric effect in an in-plane switching (IPS) liquid crystal cell for low-power consumption display devices, Sci. Rep. **6**, 35254 (2016).
[32] H. Chen, F. Peng, M. Hu, and S.-T. Wu, Flexoelectric effect on image flickering of fringe field switching LCDs, SID Symp. Dig. Tech. Pap. **47**, 274 (2016).
[33] M. Kim, H. G. Ham, H.-S. Choi, P. J. Bos, D.-K. Yang, J. H. Lee, and S. H. Lee, Flexoelectric in-plane switching (IPS) mode with ultra-high-transmittance, low-voltage, low-frequency, and a flicker-free image, Opt. Express **25**, 5962 (2017).
[34] M. S. Kim, P. J. Bos, D.-W. Kim, C.-M. Keum, D.-K. Yang, H. G. Ham, K.-U. Jeong, J. H. Lee, and S. H. Lee, Field-symmetrization to solve luminance deviation between frames in a low-frequency-driven fringe-field switching liquid crystal cell, Opt. Express **24**, 29568 (2016).
[35] I. Dozov, P. Martinot-lagarde, G. Durand, I. Dozov, P. Martinot-lagarde, and G. D. Flexoelectrically, Flexoelectrically controlled twist of texture in a nematic liquid crystal, J. Phys. Lett. **43**, 365 (1982).
[36] I. Dozov, P. Martinot-lagarde, and G. Durand, Conformational flexoelectricity in nematic liquid crystals, J. Phys. Lett. **44**, 817 (1983).
[37] G. E. A. Durand, P. Martinot-Lagarde, and I. Dozov, U.S. patent No. 4564266 (14, January, 1986).
[38] O. Elamain, G. Hegde, and L. Komitov, Polar flexoelectric in-plane and out-of-plane switching in bent core nematic mixtures, Jpn. J. Appl. Phys. **55**, 071701 (2016).
[39] G. Zheng and Z. Zhang, Flexoelectric effect in a HAN-IPS cell, Mol. Cryst. Liq. Cryst. **528**, 103 (2010).
[40] G. Zheng, H. Zhang, W. Ye, Z. Zhang, H. Song, and L. Xuan, Determination of the flexoelectric coefficient ($e1$–$e3$) in nematic liquid crystal by using fully leaky optical-guided mode, AIP Adv. **6**, 025011 (2016).
[41] D. Chen, J. H. Porada, J. B. Hooper, A. Klittnick, Y. Shen, M. R. Tuchband, E. Korblova, D. Bedrov, D. M. Walba, M. A. Glaser, J. E. Maclennan, and N. A. Clark, Chiral heliconical ground state of nanoscale pitch in a nematic liquid crystal of achiral molecular dimers, Proc. Natl. Acad. Sci. U.S.A. **110**, 15931 (2013).
[42] V. Borshch, Y.-K. Kim, J. Xiang, M. Gao, A. Jákli, V. P. Panov, J. K. Vij, C. T. Imrie, M. G. Tamba, G. H. Mehl, and O. D. Lavrentovich, Nematic twist-bend phase with nanoscale modulation of molecular orientation, Nat. Commun. **4**, 271 (2013).
[43] J. Xiang, Y. Li, Q. Li, D. A. Paterson, J. M. D. Storey, C. T. Imrie, and O. D. Lavrentovich, Electrically tunable selective reflection of light from ultraviolet to visible and infrared by heliconical cholesterics, Adv. Mater. **27**, 3014 (2015).
[44] M. Cestari, S. Diez-Berart, D. A. Dunmur, A. Ferrarini, M. R. de la Fuente, D. J. B. Jackson, D. O. Lopez, G. R. Luckhurst, M. A. Perez-Jubindo, R. M. Richardson, J. Salud, B. A. Timimi, and H. Zimmermann, Phase behavior and properties of the liquid-crystal dimer 1″,7″-bis(4-cyanobiphenyl-4′-yl) heptane: A twist-bend nematic liquid crystal, Phys. Rev. E **84**, 031704 (2011).
[45] C. Meyer, G. R. Luckhurst, and I. Dozov, Flexoelectrically Driven Electroclinic Effect in the Twist-Bend Nematic Phase of Achiral Molecules with Bent Shapes, Phys. Rev. Lett. **111**, 0067801 (2013).
[46] A. Ferrarini, C. Greco, and G. R. Luckhurst, On the flexoelectric coefficients of liquid crystal monomers and dimers: A computational methodology bridging length-scales, J. Mater. Chem. **17**, 1039 (2007).
[47] H. J. Coles, M. J. Clarke, S. M. Morris, B. J. Broughton, and A. E. Blatch, Strong flexoelectric behavior in bimesogenic liquid crystals, J. Appl. Phys. **99**, 034104 (2006).
[48] C. B. Sawyer and C. H. Tower, Rochelle salt as a dielectric, Phys. Rev. **35**, 269 (1930).
[49] T. Mitsui, I. Tatsuzaki, and E. Nakamura, *An Introduction to the Physics of Ferroelectrics* (Gordon and Breach Science Publishers, New York, 1976).
[50] Z.-Y. Cheng, Q. M. Zhang, and F. B. Bateman, Dielectric relaxation behavior and its relation to microstructure in relaxor ferroelectric polymers: High-energy electron irradiated poly(vinylidene fluoride–trifluoroethylene) copolymers, J. Appl. Phys. **92**, 6749 (2002).
[51] See Supplemental Material at http://link.aps.org/supplemental/10.1103/PhysRevApplied.8.054033 for how the Sawyer-Tower circuit is used to measure the electric polarization induced by the deformations in the liquid-crystal cell.
[52] A. Varanytsia and L.-C. Chien, Giant flexoelectro-optic effect with liquid crystal dimer CB7CB, Sci. Rep. **7**, 41333 (2017).